Vol 58, No 2—May 2024

ANALOG DEVICES | ADI Analog Dialogue™

Unleashing Cost-Efficiency with Post-PA Hybrid Beamforming in mMIMO Systems

Dmitrii Prisiazhniuk, Staff Engineer, Field Applications, and
Sinan Alemdar, Principal Engineer, Product Applications

Abstract

In order to facilitate extensive radio deployments, the low cost of the radio system and high power efficiency are key considerations for operators. Hybrid beamforming (HBF) is an effective way to address these design targets. This article describes a new post power amplifier (post-PA) HBF architecture applied to massive multi-input multi-output (mMIMO) radio systems. It presents an effective solution for the post-PA phase shifting block using two Analog Devices ADRF5347 SP4T switches, enabling the reduction of total system cost, while meeting the requirements of the mMIMO system. While this article discusses mMIMO radio, the post-PA HBF approach is generalized and can be applied to different types of radio communications (small cells, macro, mmWave, satellites), radar applications (industrial, automotive, military), or radio frequency sensing/imaging applications.

Introduction

In the past decade, globalization trends have led to a significant increase in data exchange and the use of video calls. Alongside this, the rise of digitalization and automation has created multiple new applications for 5G communication in various fields like IoT, logistics, manufacturing, transportation, and healthcare, among others. Recent data indicates that mobile data traffic is growing at an impressive 22% rate,[1] and this upward trend is expected to continue. To help operators expand, the main factors for developing and upgrading radio networks are the system's capacity, cost per bit, and power per bit.

There are three primary factors impacting the capacity of the radio system: signal bandwidth (BW), signal-to-noise ratio (SNR), and spatial multiplexing (effective number of parallel streams M sharing the same frequency resources). While SNR

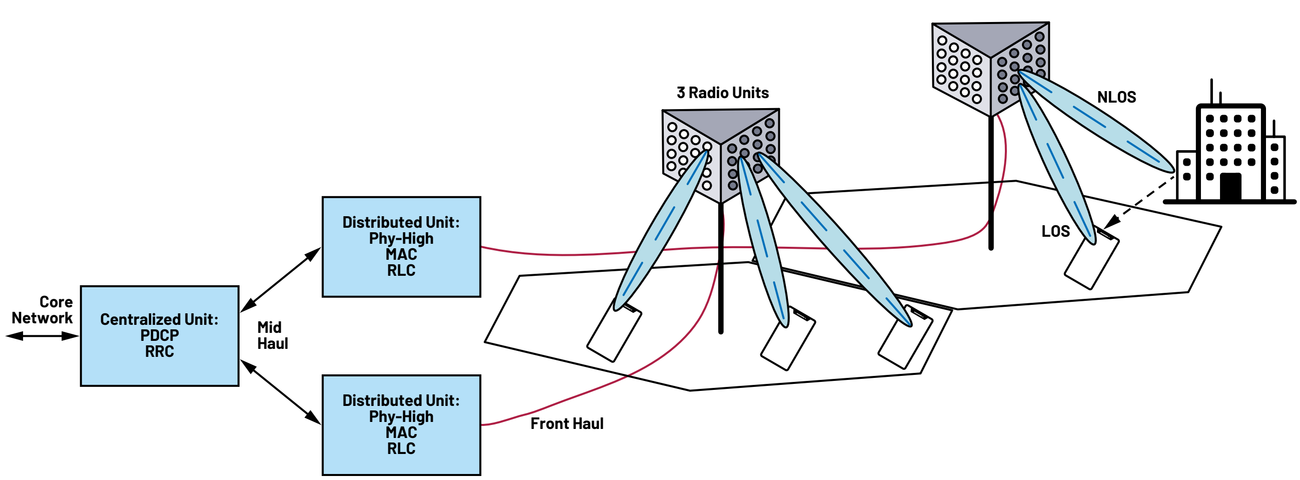

Figure 1. mMIMO radio system.

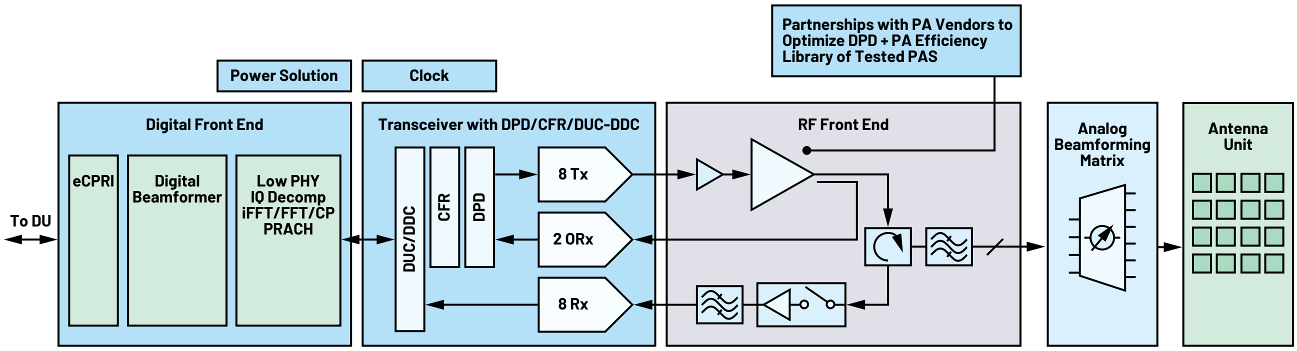

Figure 2. Typical architecture of mMIMO system.

exhibits a logarithmic dependence and typically increases the total power consumption of the system. The most substantial contributors to capacity are the BW and spatial multiplexing.

$$C = M \times BW \times Log_2 (1 + SNR) \tag{1}$$

In the past, radio development primarily focused on optimizing the utilization of time and BW resources. The advent of mMIMO leverages spatial dimension. The concept of spatial multiplexing enables concurrent communication with multiple mobile station receivers simultaneously within the same time-frequency resources. Utilizing the spatial dimension offers the potential for a significant increase in capacity, aligning with the 5G standard's target of achieving a 3-fold to 5-fold capacity increase.[2]

Figure 1 depicts a typical hexagonal cell with three mMIMO radio units (RUs) installed on the same tower, each covering 120°. Each mMIMO RU has the capability to create multiple beams for communication, either with multiple user equipment (UE) devices or with the same UE through multiple beams, effectively reaching the UE via different propagation paths (for example, line-of-sight and non-line-of-sight reflected from a building). On the other side, the RU is typically connected to the distributed unit (DU) and centralized unit (CU), which are responsible for resource management and are connected to the core mobile network.

While mMIMO systems offer significantly higher capacity, they typically operate over shorter distances. This limitation arises from the need for higher frequencies to enable the use of narrower beams and associated path losses. Even though losses can be partially reduced through more focused narrower beams achieved by higher antenna gain, this approach still reduces the overall coverage range of the radio system. Consequently, to utilize mMIMO systems efficiently, it becomes necessary to deploy multiple mMIMO radio systems, a phenomenon referred to as densification. Densification is particularly relevant for applications in highly populated environments such as cities with high capacity needs and many users. Operators are likely to deploy a significant number of mMIMO systems in urban areas if the system's cost is low enough, with cost-effectiveness being a crucial factor driving the development of mMIMO technology.

Figure 2 represents a typical RU architecture consisting of five main blocks: the digital front-end unit (DFE), transceiver unit (TRX), RF front-end (RFE) unit, analog beamforming matrix, and antenna unit.

The DFE encompasses blocks responsible for managing the DU interfaces, digital beamforming, and low PHY processing.

The TRX converts digital IQ samples generated by the DFE into the RF domain within a specified frequency range. ADI transceivers go beyond converting IQ samples into the RF domain; they incorporate a digital engine featuring digital predistortion (DPD) and crest factor reduction (CFR) algorithms, along with digital upconverters/downconverters (DUC/DDC). DPD enhances power amplifiers (PA) efficiency, allowing PAs to operate at higher power levels.[3] This results in an overall improvement in the power efficiency of the radio system. ADI is also partnering with major PA vendors to evaluate their performance and develop the most optimal DPD solution. A recent example of a transceiver with DPD capabilities is ADI's ADRV9040, which linearizes signals up to 400 MHz BW.

The RFE unit amplifies the RF signal to the required level for transmission on the transmitter side or for reception by the transceiver on the receiver side. Table 1 features solutions that can be employed for this application.

Table 1. ADI RFE Solutions Used in mMIMO System

TX VGA	ADL6337, ADL6317
LNA with Integrated Switch	ADRF5519, ADRF5515A, ADRF5534, ADRF5532
ORX Switch	ADRF5250, HMC8038

An antenna unit typically consists of a large number of antenna elements (AE). Modern mMIMO systems can incorporate as many as 128 to 384 AEs, distributed both horizontally and vertically, as well as utilizing two different polarizations. For instance, an antenna array with 128 elements could be structured as 8 × 8 × 2 (eight elements in vertical directions, eight in the horizontal, and two polarizations), while an antenna array with 192 elements can be structured as 12 ×8 × 2.[2,4] Constructing many active elements, such as transceiver channels and amplifiers, is not feasible due to the exorbitant costs it would involve. To address this challenge, a solution is to map all of the AEs (for example, 128 to 384 AEs) to a smaller number of amplifying units—for example, to 16, 32, or 64 RFEs. This can be achieved using an analog beamforming matrix, which includes splitters and optionally phase shifters. The primary focus of this article is the hybrid beamforming approach, which combines both digital and analog beamforming, and how it can reduce the overall system cost with SP4T switchers.

Hybrid Beamforming in mMIMO Systems

The fundamental idea behind mMIMO involves creating multiple narrow beams that can be directed toward UE. These beams are formed by either activating the AEs with a shared signal source on the transmitter side or by combining them on the receiver side. In the far-field region, the radiating electric fields produced by these sources combine, leading to either constructive or destructive interference patterns. The beam shape of the combined source can be controlled by adjusting the phases, separations, and amplitudes of individual sources. In a simplified form, the antenna gain of the combined array can be described as:

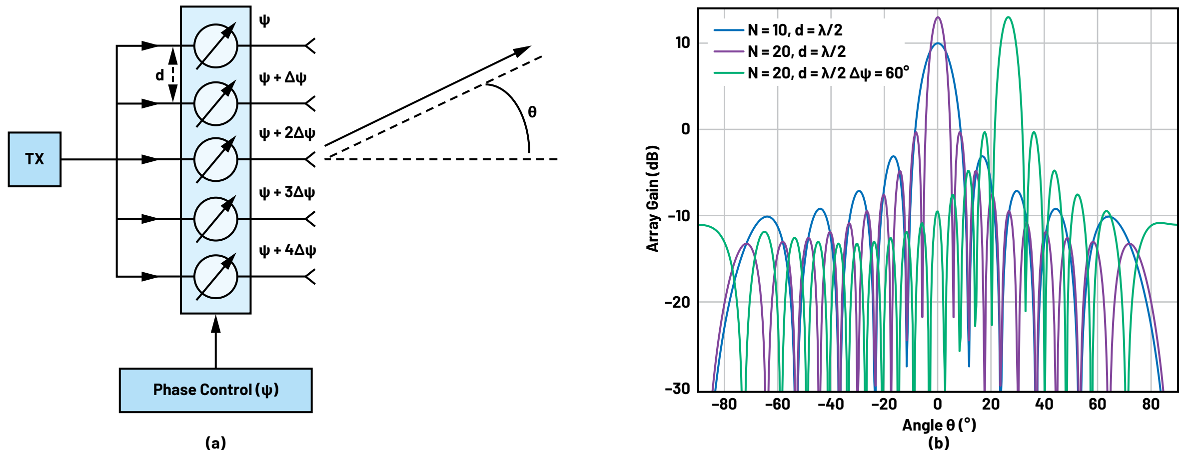

Figure 3. (a) Schematic representation of beamforming; (b) example of the array gain for 10 and 20 elements (purple and blue) as well as after applying phase shift of 60° between each pair of antennas (green).

$G_{comb}(\theta,\varphi) = |AF(\theta,\varphi)|^2\, G_{AE}(\theta,\varphi)$, where G_{AE} represents the antenna gain of an individual antenna element, and $AF(\theta,\varphi)$ denotes the array factor (AF). Here, θ and φ correspond to the vertical and horizontal angles, respectively. For a more detailed explanation of how the antenna array pattern is formed, refer to "Phased Array Antenna Patterns—Part 1: Linear Array Beam Characteristics and Array Factor."[4] For simplification purposes, a one-dimensional array with antennas separated by distances d and phase shifts Δψ applied between each pair of antennas is considered, as illustrated in Figure 3a. In this case, AF can be calculated using the following equation.

$$|AF(\theta)|^2 = \frac{1}{N}\left|\frac{\sin\left(N\left[\frac{\pi d}{\lambda}\sin\theta - \frac{\Delta\Psi}{2}\right]\right)}{\sin\left(\frac{\pi d}{\lambda}\sin\theta - \frac{\Delta\Psi}{2}\right)}\right|^2 \qquad (2)$$

Figure 3b shows examples of array gain for 10 and 20 antenna elements (purple and blue) with half-wavelength separation between antennas. The green curve demonstrates the beam after applying phase shifts ΔΨ of 60° between each pair of antennas, which results in a beam angle of approximately 26.5°.

The 3 dB beamwidth can be approximated using the following expression: $\Delta_{\varphi 3db}[rad] = 0.886 \times \lambda/Nd$. For instance, assuming an operation at 3.5 GHz, with half-wavelength spacing and a total of eight elements (typically representing horizontal beamforming), the beamwidth would be approximately 12°. This relationship underscores why mMIMO finds its practical application predominantly in the middle frequency range of 2.5 GHz to 4 GHz. For lower frequencies, such as 1 GHz, achieving the same beamwidth would require significantly larger antenna sizes, making such systems impractical for deployment. There are constraints on the weight and size of the mMIMO radio, in order that a single person can easily lift and install the radio.

The size of the antenna and the number of AEs depend on the beamwidth requirements and frequency of operation. Present-day mMIMO systems can incorporate a total of 128 to 384 AEs. It's worth noting that the spacing in the horizontal and vertical directions between antennas can be different, driven by different requirements of the beamwidth and the maximum/minimum angle of scanning. For example, in vertical domains, where the number of users is limited, it is feasible to restrict both the vertical range and the number of vertically supported beams to a small quantity.

For a mMIMO system, it is essential that all AEs sharing the same transmit/receive UE data stream vary only in phase and possibly gain. There are multiple ways this can be implemented as shown in Figure 4.

Figure 4a illustrates the simplest form of beamforming, known as pure analog beamforming. In this configuration, a small amount of data streams is connected to transceivers and power amplifiers. Amplified RF signals are then split and phase-rotated before being connected to different AEs. In this configuration, the number of TRX converters and amplifiers matches the number of required data streams ($N_{TRX} = N_{PA} = N_{STR}$), while the number of phase shifters is a product of both the number of streams and unique active pipes ($N_{PH} = N_{STR} \times N_{PIPE}$). Each pipe can be connected to multiple AEs (AE_1, … AE_K). Although this architecture reduces the number of TRX converters and amplifiers, its limitation lies in the number of simultaneously supported UE devices. To scale the system for many users, a substantial number of phase shifters and a complex splitting/combining network would be necessary. Moreover, beam sweeping would be required to provide coverage across a wider area. However, this approach becomes relevant for millimeter wave (mmWave) radio, where the requirement is to accommodate a smaller number of users.

Digital beamforming (Figure 4b) has become one of the most popular architectures largely in part due to the limited number of UE devices supported by analog beamforming. In this approach, data streams are divided and phase-rotated directly in the digital domain before being converted to the RF domain through transceivers. The major advantage of this approach lies in its flexibility, as it can support a scalable number of users. However, the digital overhead in the DFE required to support every pipe, as well as the number of converters and amplifiers needed to support every pipe ($N_{TRX} = N_{PA} = N_{PIPE} > N_{STR}$) results in increased system cost and power consumption.

Hybrid beamforming (Figure 4c) represents an approach to address the system cost of mMIMO. In this architecture, beamforming is divided between the digital and analog domains. A potential split could entail digitally controlling the beam exclusively in the horizontal plane while executing it in an analog manner (or a

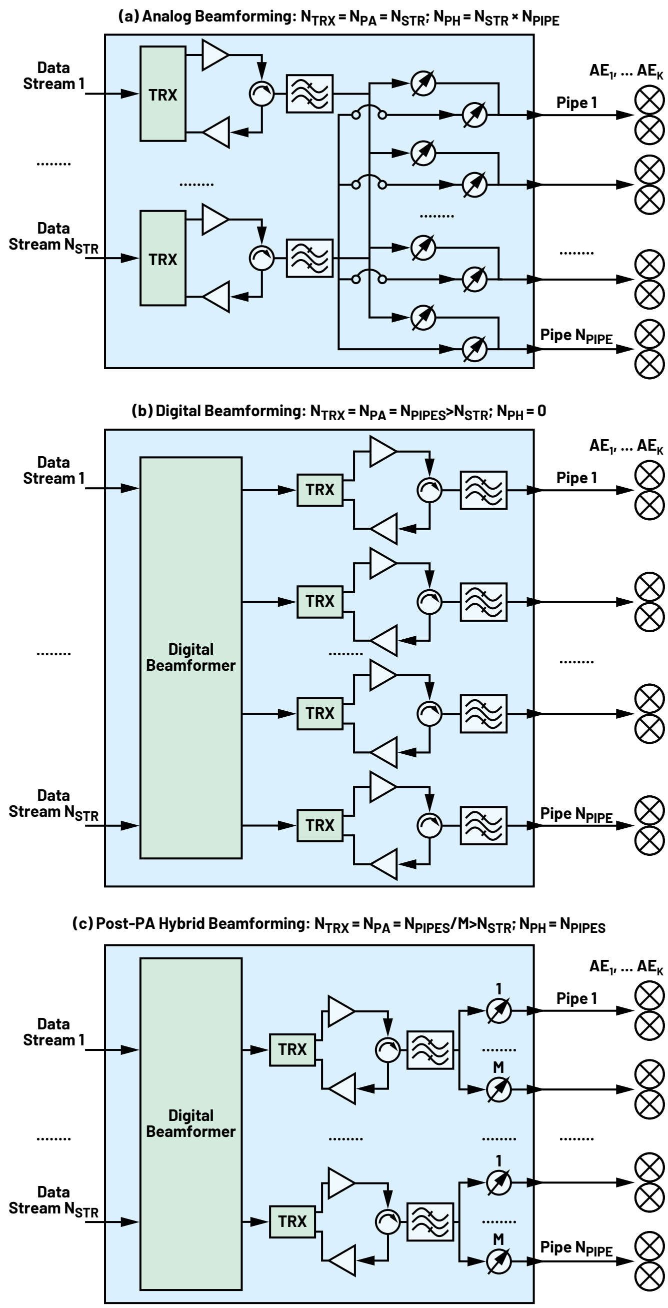

Figure 4. Comparison of (a) analog, (b) digital, and (c) post-PA hybrid beamforming schemes.

combination of digital and analog) in the vertical domain. This approach is justified because there are typically a limited number of users located at various vertical angles. By implementing the split in both the digital and analog domains, cost reduction is achieved due to the reduced number of RF chains ($N_{TRX} = N_{PA} = N_{PIPE}/M$, where M is the split factor) while maintaining a reasonable number of beams and flexibility. At the same time, this approach would require additional phase shifters in front of pipes ($N_{PH} = N_{PIPE}$), which results in associated cost and power loss on components. Another possible benefit of this architecture is decreased power consumption in both the DFE and transceivers because of the reduced number of chains being utilized.

In Figure 4c, the phase shifter is placed after the power amplifier and is referred to as the post-PA HBF architecture. This approach offers distinct advantages compared to the pre-PA HBF architecture, where the splitting and the phase shifting happen before the PA. A comparison of these two architectures is shown in Table 2.

Table 2. Comparison of Post-PA and Pre-PA Phase Shifting Approaches

	Post-PA Phase Shifting	Pre-PA Phase Shifting
Advantages	1. Require a small amount of PAs/LNAs and circulators 2. Only a single PA needs to be linearized via DPD using the same TRX signal 3. Phase shifter can be integrated very close to antenna elements	1. Insensitivity to the insertion loss of the phase shifter on the system level 2. Phase shifters need to handle rather low power 3. RX noise figure of chain is lower
Disadvantages	1. Phase shifters need to handle high power and have very high IP3 performance 2. Phase shifter should have very low insertion loss, as every dB of power loss results in an efficiency drop in the radio 3. RX noise figure of chain is higher	1. Multiple PAs need to be linearized via DPD using the same signal 2. Require a higher number of PAs/LNAs

Therefore, the post-PA HBF architecture brings benefits with fewer components, but at the expense of increased demands on linearity, required power levels, and the insertion loss of the phase shifter.

Requirements for Phase Shifters

To enable the post-PA hybrid beamforming application, it is essential to meet the beam management requirements of the 5G standard as well as to satisfy mMIMO system constraints.

Switching Time

5G deploys orthogonal frequency division multiple access (OFDMA) as the transmission engine for data. OFDMA enables the allocation of independent modulating subcarriers within the total bandwidth, facilitating the efficient scaling of resources to accommodate varying number of users and their corresponding data requirements.

The 5G standard defines a transmission of data in frames (each lasting 10 ms) consisting of 10 subframes (each lasting 1 ms). It introduced the concept of flexible numerology, allowing the utilization of a variable number of slots within a single subframe. The length and number of slots scale with subcarrier spacing, as indicated in Table 3. These slots define the fundamental transmission unit referred to as a resource grid, consisting of 12 subcarriers and 14 OFDMA symbols each.

The duration of each OFDMA symbol consists of the primary data block and an additional cyclic prefix block. The cyclic prefix mitigates intersymbol interference arising from signal propagation via various paths (multipaths). It essentially involves the cyclic repetition of the same signal and is typically removed during processing to prevent overlapping of different symbols. The cyclic prefix time interval is ideal for beam switching, as no data is transmitted during this period. For the FR1 standard (sub-6 GHz applications), the minimum cyclic prefix duration is set at 1.17 µs, and this duration fundamentally defines the switching time that a phase shifter should support (see Table 3).

Table 3. 5G Cyclic Prefix Time Depending on Selected Numerology

Standard	Subcarrier Spacing	Slot Length	Symbol Time	Cyclic Prefix Time
FR1	15 kHz	1 ms	66.7 µs	4.69 µs
FR1	30 kHz	0.5 ms	33.3 µs	2.34 µs
FR1/FR2	60 kHz	0.25 ms	16.7 µs	1.17 µs
FR2	120 kHz	0.125 ms	8.33 µs	0.59 µs
FR2	240 kHz	0.0625 ms	4.17 µs	0.29 µs

Power Level Handling

In a typical mMIMO system, the average total transmitting power output is approximately 55 dBm (320 W). Assuming that this power is divided among 32 active transmission pipes, this results in an allocation of approximately 40 dBm average power per amplifier. The power that passes through the phase shifter varies depending on the number of power splits utilized as summarized in Table 4.

Table 4. Power Handling of Phase Shifter Requirements

	Average Power in Phase Shifter	Peak Power Assuming Peak-to-Average Ratio of 8 dB
1-to-2 split	37 dBm	45 dBm
1-to-4 split	34 dBm	42 dBm

Linearity

The signal passing through the phase shifter should not be disturbed due to nonlinear third-order intermodulation mechanisms. The intermodulation products should not exceed a certain limit after the power amplifier and the bandpass filter. The input intercept point (IIP3) parameter of the phase shifter will define the third-order intermodulation distortion (IM3) of the device. Achieving intermodulation products below –60 dBm with an incident power of 37 dBm necessitates a minimum IIP3 of 81 dBm.

$$IIP3 = \frac{3 \times (Ptotal - 3) - IM3}{2} \tag{3}$$

Insertion Loss

As the phase shifter is positioned between the PA-LNA front end and the antenna, its insertion loss directly impacts the transmitted power during transmission and the overall system noise figure during receive operations. For instance, assuming the phase shifter incurs a 3 dB insertion loss, the consequence would be a 50% power loss, rendering the system highly inefficient. The benefits of HBF, which include reducing DFE and TRX power consumption, should be carefully weighed against the added power loss introduced by HBF. Improvements in the insertion loss of the phase shifter will enhance the radio's efficiency, consequently reducing operational costs for mMIMO radios—a crucial parameter for operators.

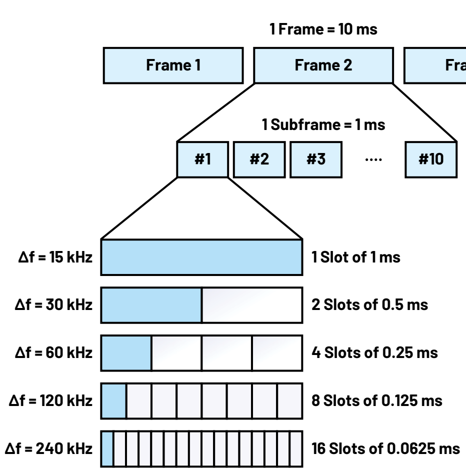

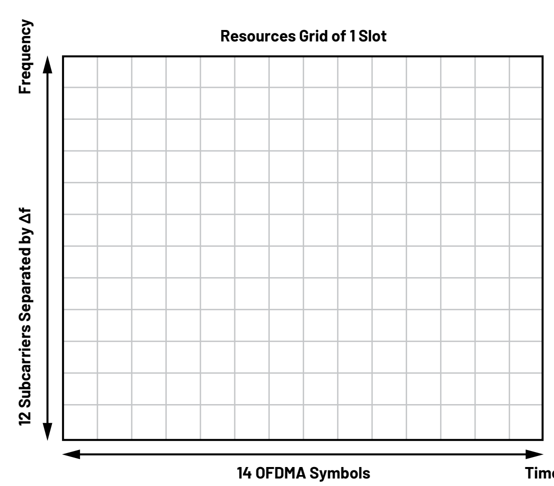

Figure 5. 5G data frame structure.

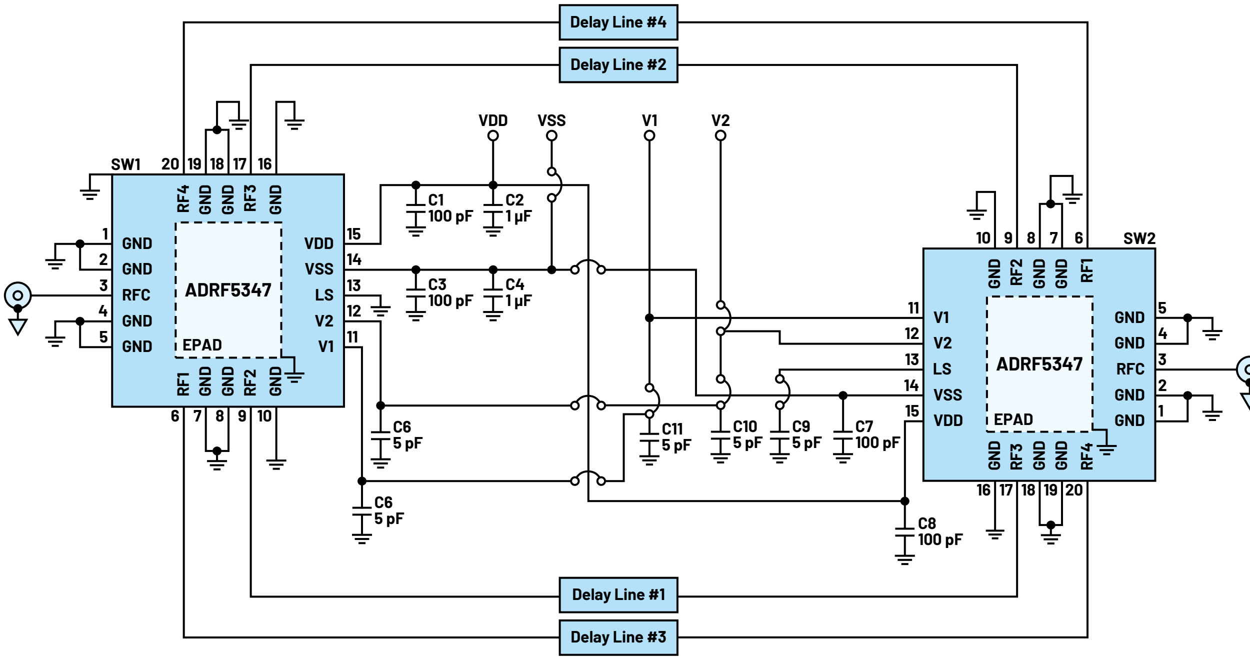

Figure 6. Switched-line phase shifter implementation using back-to-back SP4T switches.

Control		SW#1		SW#2		Phase
V1	V2	LS	Ch	LS	Ch	
0	0	0	RF1	1	RF4	Delay Line #3 (–60°)
1	0	0	RF2	1	RF3	Delay Line #1 (Ref)
0	1	0	RF3	1	RF2	Delay Line #2 (–30°)
1	1	0	RF4	1	RF1	Delay Line #4 (–90°)

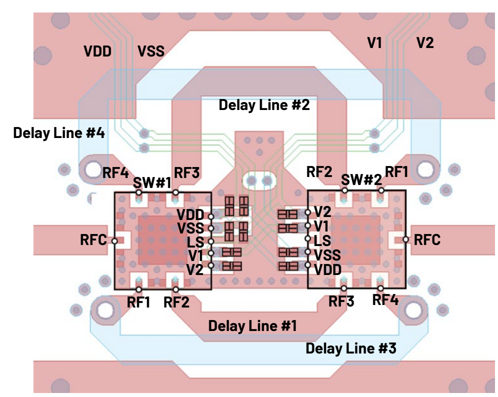

Figure 7. Reference back-to-back phase shifter design using SP4T switches.

Cost

An additional component in HBF architecture is the phase shifter. For this architecture to be more economically appealing, the cost of additional phase shifters ($Cost_{PS}$) and PCB splitting networks ($Cost_{SN}$) should be lower when compared to the savings achieved by reducing the number of transceiver channels and power amplifiers ($Cost_{TRX}$ + $Cost_{PA}$), as shown in Equation 4.

$$(Cost_{PS} + Cost_{SN}) < (Cost_{TRX} + Cost_{PA}) \times \left(1 - \frac{1}{M}\right) \tag{4}$$

Where M is the splitting factor. For a 1-to-2 split configuration, the combined cost of the phase shifter and splitting network should be less than half the cost of the PA and TRX. Anticipating the next generation of systems operating around ~7 GHz, a potential increase in the number of transceiver units by a factor of four is expected compared to existing mMIMO systems at ~3.5 GHz. Therefore, the cost-saving factor provided by the post-PA phase shifter is projected to be a pivotal factor in enabling next-generation deployments.

Cost-Effective Phase Shifters Using Two SP4T Switches

As highlighted in Table 2 and the requirements section, the effectiveness of post-PA phase shifter methods depends on achieving minimal insertion loss and excellent linearity (intermodulation performance). The goal is to maximize the radiated power with minimal distortion. Traditional on-chip phase shifters face challenges in simultaneously achieving low insertion loss and high linearity. The primary contributor to the loss issue is the inherent resistance of on-chip metal and the presence of lossy dielectric materials, in contrast to the implementation of a delay line on a low loss PCB substrate. While it is possible to optimize the loss component on-chip, achieving high linearity is a challenge because these two parameters exhibit an inverse relationship in current on-chip phase shifter approaches.

Creating a four-step phase shifter on a low-loss substrate involves configuring two SP4T switches in a back-to-back arrangement. Each RF arm of the SP4T switches is interconnected through RF traces with varying physical lengths, resulting in distinct time delays, and consequently, a phase shift at the desired frequency. To prevent the phase errors of the overall structure, the SP4T switches should provide decent isolation (that is, >20 dB) in the required frequency band. Among the four delay lines, one is designated as the reference delay line, while the

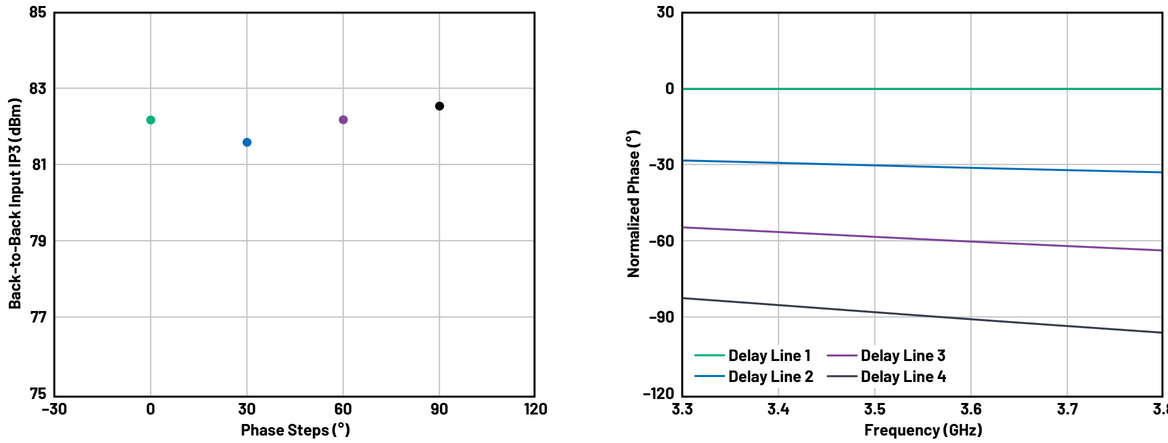

Figure 8. Phase steps and end-to-end OIP3.

remaining three lines introduce additional phase shifts that are normalized to the reference delay line, as depicted in Figure 6. Since these delay lines are printed on a PCB, the phase steps are inherently more resistant to component variations.

The relative phase shift can be determined by comparing the physical length difference between one of the delay lines and the reference line, as expressed in the equation below:

$$\Delta\Psi = 2\pi\left(\frac{\Delta L}{\lambda}\right) \quad (5)$$

In this equation, ΔL represents the difference in physical lengths between the two delay lines, and λ denotes the wavelength on the PCB. This equation indicates that the phase shift is anticipated to exhibit a linear relationship with frequency, making it feasible to scale this method across various frequencies or broad bandwidths with ease.

This approach imposes specific requirements, including the simultaneous attainment of low insertion loss, high RF power handling, high IP3 performance, and rapid switching speeds for the SP4T switches employed in this context. Achieving this combination of attributes is a challenging task, however, ADI's high linearity SP4T ADRF5347 meets these demands. It offers a 0.4 dB insertion loss at 3.6 GHz, all while maintaining an input IP3 rating exceeding >84 dBm. Moreover, it demonstrates an RF power handling capability with an average of 37 dBm and a peak of 47 dBm, making it suitable for handling complex communication signals known for their high peak-to-average ratios. Notably, its switching event completes ~700 ns, a feature enabled by its patented design, matching the rigorous demands of 5G radio standards.

The back-to-back SP4T phase shifter can be efficiently implemented in terms of space, as illustrated in Figure 7. In this reference design, 30° phase increments are achieved at 3.6 GHz. The SP4T components measure 4 mm × 4 mm, with a 4 mm separation between the two parts, where supply and control capacitors can be densely populated. Instead of individual control for each SP4T switch, they can be programmed with inverted logic, enabling both switches to be controlled using the same set of control lines. For instance, when the first switch selects the RF1 arm, the second switch simultaneously chooses the RF4 arm, all through the same control logic. This space-efficient phase shifter module can be replicated across all antenna elements.

The design is realized on the Aerowave AW-300, which shows inherent low passive intermodulation products and low RF loss characteristics, making it well-suited for this application. The selection of the RF substrate carries significance not only in terms of minimizing losses but also in potentially influencing the overall end-to-end IP3, especially when its passive intermodulation properties are not excessively high. For a single SP4T ADRF5347, the input IP3 typically exceeds 84 dBm, and when two of these SP4T switches are linked in a cascading configuration, the resulting end-to-end IP3 performance is achieved at levels greater than 81 dBm across all phase line selections, as demonstrated in Figure 8.

Switching between various delay lines is a straightforward method for achieving the desired phase shift. However, it's essential to obtain minimal difference in the insertion loss and return loss among these four different lines, as such variations are undesirable. The SP4T switches are expected to exhibit excellent insertion loss and return loss for every phase selection to ensure robust cascaded performance. As depicted in Figure 9, the insertion loss remains within the range of ±0.025 dB at 3.6 GHz, and the return loss is better than 24 dB for all phase selections. This performance is attributed to the combination of low insertion loss and the excellent return loss offered by all RF channels of the SP4T switch (ADRF5347).

Conclusion

In conclusion, SP4T switch-based phase shifters, leveraging the HBF approach, greatly reduce the cost of mMIMO systems. ADI's ADRF5347 effectively addresses the challenges of post-PA phase shifters, including insertion loss, high linearity, and robust power handling. The low insertion loss of the switch directly contributes to the power efficiency of the radio, thereby mitigating power-related operational costs for operators.

Operating across the 1.8 to 3.8 GHz range, the ADRF5347 caters to various mMIMO applications within this frequency spectrum. With mMIMO systems anticipated to extend up to 7.125 GHz in the future, the principles presented in this article provide a solid foundation for scalability. Importantly, the adaptability of the ADRF5347 extends beyond mMIMO applications, with the potential to enhance phase shifters for beamforming in diverse radio systems such as small cells, macro radio, mmWave, and satellite communications.

Furthermore, this innovative approach is not limited to traditional communication systems alone; its applicability extends to radar applications and radio frequency sensing/imaging, demonstrating the versatility of HBF in addressing challenges across a spectrum of cutting-edge technologies. In essence, it paves the way for cost-effective, efficient, and scalable solutions with broad-reaching implications across the field of wireless communications and beyond.

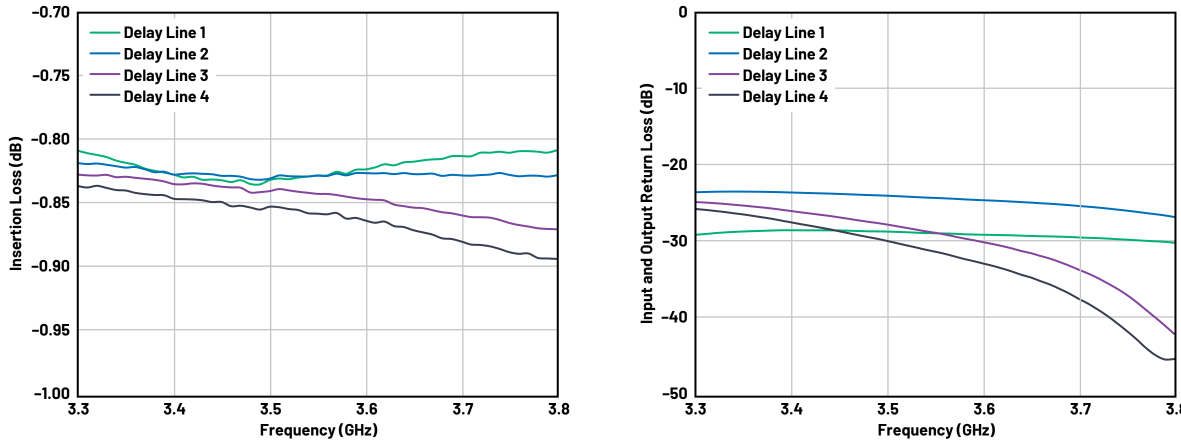

Figure 9. Insertion loss and return loss performance for back-to-back phase shifter.

References

[1] *Ericsson Mobility Report*. Ericsson, 2024.

[2] "Extreme Massive MIMO for Macro Cell Capacity Boost in 5G-Advanced and 6G." Nokia Bell Labs, October 2021.

[3] Claire Masterson. "Digital Predistortion for RF Communications: From Equations to Implementation." *Analog Dialogue*, Vol. 56, April 2022.

[4] Peter Delos, Bob Broughton, and Jon Kraft. "Phased Array Antenna Patterns—Part 1: Linear Array Beam Characteristics and Array Factor." *Analog Dialogue*, Vol. 54, May 2020.

Advanced Antenna Systems for 5G. 5G Americas, August 2019.

About the Author

Dmitrii Prisiazhniuk is a staff field application engineer at Analog Devices in Munich, Germany, responsible for customer support and the development of radio, optical, and cloud infrastructure communication applications. He has approximately 15 years of experience across RF, optical, and power fields. Before joining ADI in 2021, he held a position in system engineering, where he was responsible for the development of automotive mmWave radars. Dmitrii holds a Ph.D. degree from the Technical University of Munich and an M.B.A. degree from Quantic School of Business and Technology.

About the Author

Sinan Alemdar is currently employed as a principal application engineer in ADI's Microwave Communications Group, working from the Istanbul Design Center. He provides application support for a range of RF products, including switches, attenuators, and front ends. He became a part of Analog Devices in 2016, following a 4-year experience in the aerospace and defense industry. Sinan holds B.S., M.Sc., and Ph.D. degrees in electrical engineering from Bilkent University.